Refractory ventricular tachycardia treated by a second session of stereotactic arrhythmia radioablation

C. Herrera Siklody [a], E. Pruvot [a,*], P. Pascale [a], R. Kinj [b], R. Jumeau [b], M. Le Bloa [a], C. Teres [a], G. Domenichini [a], A.P. Porretta [a], M. Ozsahin [b], J. Bourhis [b], L. Schiappacasse [b]

[a] Department of Cardiology, Lausanne University Hospital (CHUV) and Lausanne University (UNIL), Switzerland
[b] Department of Radiation Oncology, Department of Oncology, Lausanne University Hospital (CHUV) and Lausanne University (UNIL), Switzerland

ABSTRACT

Purpose: Stereotactic arrhythmia radioablation (STAR) is an effective treatment for refractory ventricular tachycardia (VT), but recurrences after STAR were recently published. Herein, we report two cases of successful re-irradiation of the arrhythmogenic substrate.
Cases: We present two cases of re-irradiation after recurrence of a previously treated VT with radioablation at a dose of 20 Gy. The VT exit was localized on the border zone of the irradiated volume, which responded positively to re-irradiation at follow-up.
Conclusion: These two cases show the technical feasibility of re-irradiation to control recurrent VT after a first STAR.

Introduction

Stereotactic arrhythmia radioablation (STAR) has been recently introduced as an effective treatment of ventricular tachycardia (VT) refractory to catheter ablation (CA) and antiarrhythmic drugs [1–6]. Although STAR significantly reduced VT burden, recurrences were recently reported [1–4]. So far, only 2 cases of unsuccessful re-irradiation have been published [3,6]. Herein, we present two cases of recurrent VT after a first STAR procedure that were successfully managed with a 2nd STAR.

Methods

All radiotherapies were performed with a CyberKnife® system (Accuray Inc., Sunnyvale, CA), using a Synchrony technique, in which the distal dipole of the right ventricular lead of the implanted cardiac defibrillator (ICD) was used as a fiducial, allowing real-time tracking. Velocity AI® software (Varian Medical Systems Inc., Palo Alto, California) was used for structure delineation and image registration. The ablation volume comprising the arrhythmogenic substrate (AS), which was outlined by the electrophysiologists according to the electro-anatomical mapping (EAM). Based on standard dose constraints of SBRT treatments, inverse planning was utilized to spare organs at risk (OARs)

according to the report of the AAPM [7]. Due to the lack of consensus on coronary arteries, an institutional constraint was applied based on a maximum dose (0.03 cm^3) of < 12 Gy. MultiPlan® treatment planning system was used to calculate SBRT plan. Herein, we report for the 1st time re-irradiation as bailout procedures for uncontrollable VT.

Case 1

A 73-year-old man with ischemic heart disease, a moderate aortic stenosis and a history of VT was referred to our hospital for recurrent symptomatic VT despite amiodarone. In 2012, he suffered from an inferior myocardial infarction (MI), followed three months later by an hemodynamically unstable monomorphic VT for which an ICD was implanted. In 2016, he underwent a CA for recurrent VTs and shocks. Two distinctive VT morphologies were induced: VT-A exited at the anterior basal left ventricle (LV) where it was reproduced by pace-mapping on a limited region of fragmented potentials at the anterior mitral annulus (Fig. 1A, segment 1); VT-B (not shown) exited at the basal infero-lateral LV within the MI (segments 4 and 5). Both VTs were targeted by CA. Unfortunately, VT-A recurred after a few months. As VT-A displayed a pseudo-delta wave suggestive of an epicardial exit (Fig. 1A, red arrow), a combined *epi-* and endocardial CA procedure was scheduled in November 2018. The EAM revealed no early epicardial
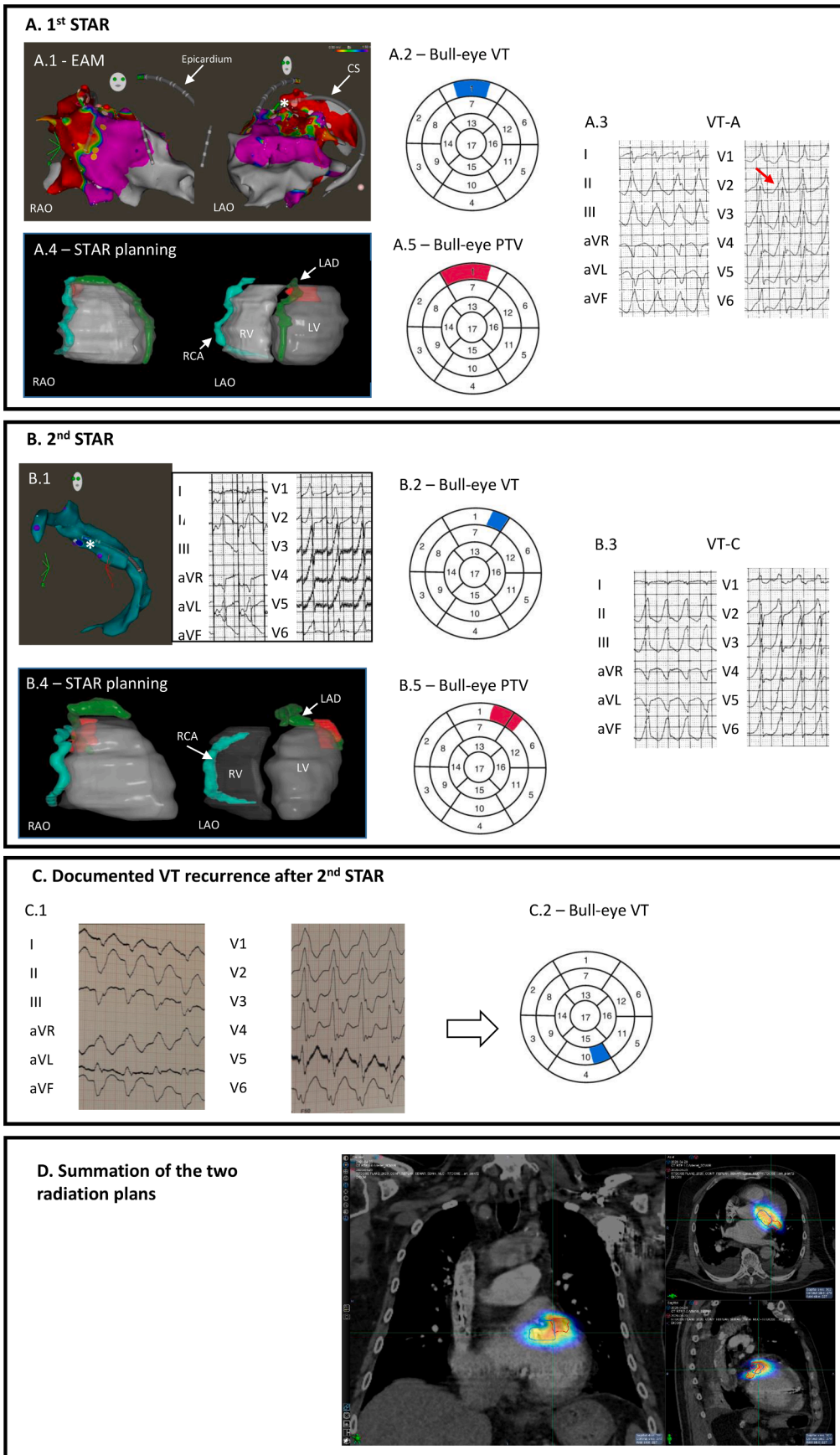
Fig. 1. Overview of the procedures for Case 1. **A.1.** Epicardial anterior VT targeted by STAR. EAM of the LV during the last CA before STAR: bipolar voltage maps in RAO (left) and RAO (right) views, with the tip of the ablation catheter (white star) located in the CS at the best pacemap spot. A decapolar diagnostic catheter is positioned epicardially facing the ablation catheter. **A.2.** Bull eye's plot displaying the VT substrate location in the 17-segment AHA model (in blue). **A.3.** 12-lead ECG of VT-A, displaying a pseudo-delta wave (red arrow) suggesting an epicardial exit. **A.4.** RAO and LAO views of the STAR plan with the PTV in red. **A.5.** Bull eye's plot displaying the location of the PTV in the 17-segment AHA model (in red). **B.1.** Second STAR procedure. EAM of the coronary sinus corresponding to the last CA before the 2nd STAR with the tip of the ablation catheter (white star) located at the best pacemap spot. Note that the ablation catheter lies more laterally as compared to its 1st location in figure 1A. Unipolar pacemapping with a guidewire is displayed on the right. **B.2.** Bull eye's plot displaying the location of the VT exit in the 17-segment AHA-model (in blue). **B.3.** 12-lead ECG of the induced VT (VT-C). **B.4.** RAO and LAO views of the STAR plan with the PTV in red. **B.5.** Bull eye's plot displaying the location of the PTV in the 17-segment AHA-model (in red). **C.** VT from the ischemic scar observed in 2022. **C.1.** 12-lead ECG and **C.2.** location on the 17-segment AHA-model (in blue) of the exit of the documented VT recurrence after the 2nd STAR procedure. RAO: right anterior oblique; LAO: left anterior oblique; CS: coronary sinus; RCA: right coronary artery; LAD: left anterior descending coronary artery: RV: right ventricle; LV: left ventricle. **D. Summation of the two radiation plans.**
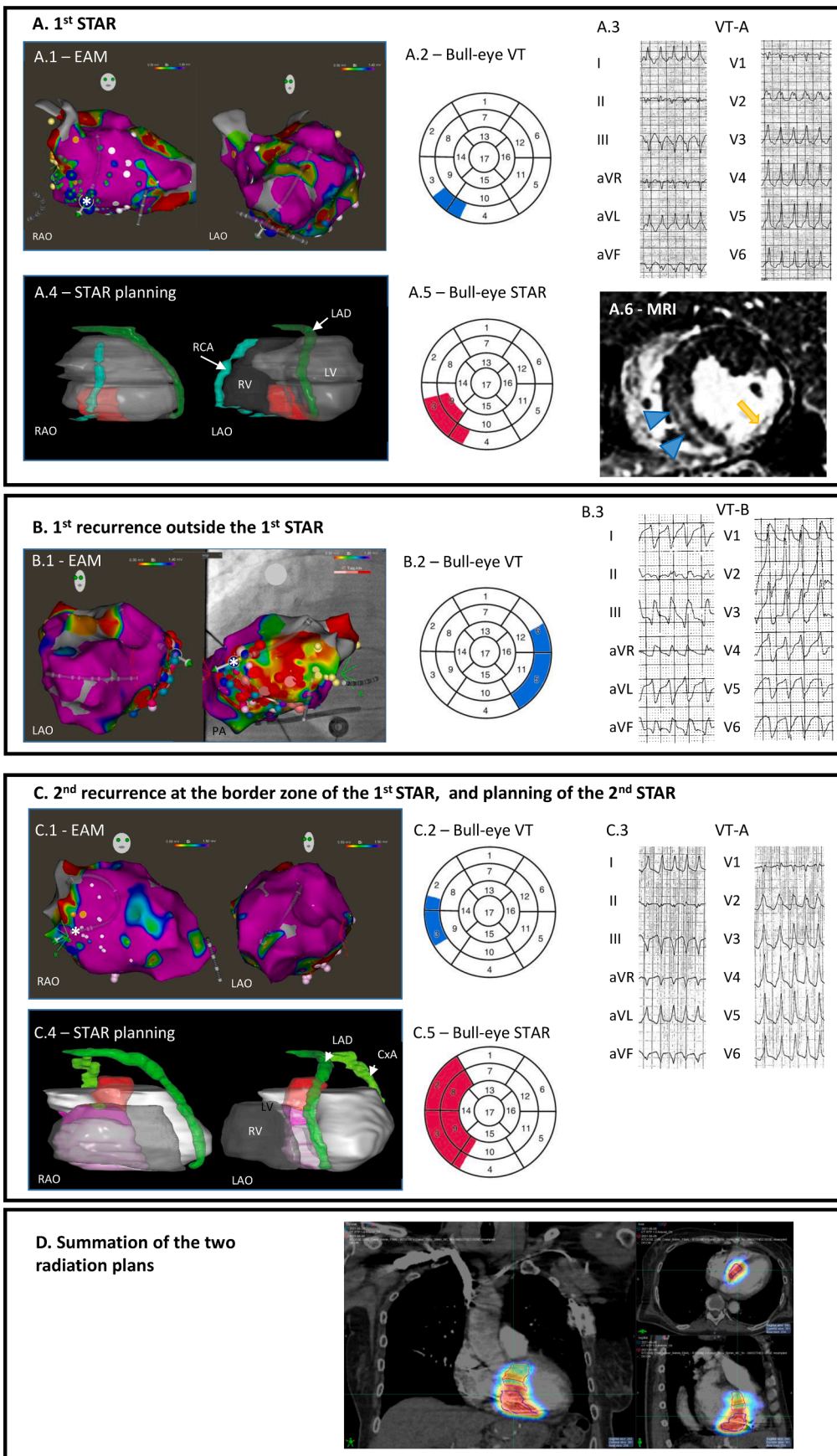
Fig. 2. Overview of the procedures for Case 2. **A.1.** VT from the septal fibrotic infiltration targeted by STAR. EAM of the LV from the last CA before STAR: bipolar voltage maps in RAO (left) and RAO (right) views, with the tip of the ablation catheter (white star) located at the best endocardial pacemap spot corresponding to the inferior basal IVS (blue tags). **A.2.** Bull eye's view displaying the exit of the VT in the 17-segment AHA-model (in blue). **A.3.** 12-lead ECG of the clinical VT (VT-A). **A.4.** 3-D reconstruction of the irradiation plan with the PTV in red. **A.5.** Bull eye's plot displaying the location of the PTV based on the 17-segment AHA-model (in red). **A.6.** Late enhancement cardiac MRI showing the fibrotic infiltration of the septum (blue arrowheads) and of the infero-lateral MI (yellow arrow). **B.1.** VT from the ischemic scar successfully treated by CA. LV EAM following the 1st VT recurrence after STAR: bipolar voltage maps in LAO (left) and PA (right) views, with the tip of the ablation catheter (white star) located at the successful ablation site. Red tags indicate ablation spots. **B.2.** Bull eye's plot displaying the location of the VT substrate in the 17-segment AHA-model (in blue). **B.3.** 12-lead ECG of the induced VT (VT-B) that differed from VT-A shown in panel A3. **C.1.** Second STAR procedure targeting the septal non-ischemic VT. LV EAM corresponding to the last CA before the 2nd STAR procedure: bipolar voltage maps in RAO (left) and RAO (right) views, with the tip of the ablation catheter (white star) located at the best endocardial pacemap spot at the intersection of the inferior and middle third of the basal IVS. **C.2.** Bull eye's plot displaying the location of VT exit in the 17-segment AHA-model (in blue). **C.3.** 12-lead ECG of the clinical VT (VT-A). **C.4.** RAO and LAO views of the STAR plan with the PTV in red and the complementary and transition volume in pink and fuchsia respectively. **C.5.** Bull eye's plot displaying the location of the new PTV in the 17-segment AHA-model (in red). RAO: right anterior oblique; LAO: left anterior oblique; PA: postero-anterior; CS: coronary sinus; RCA: right coronary artery; LAD: left anterior descending coronary artery: CxA: circumflex coronary artery; RV: right ventricle; LV: left ventricle. **D. Summation of the two radiation plans**.

potentials and endocardial RF ablation with power titration up to 50 W failed to terminate VT-A. A STAR procedure was planned on January 10, 2019 targeting the intramyocardial AS localized at segment 1 (Fig. 1A). A dose of 20 Gy (79 % prescription isodose) was delivered over a PTV of 13.57 cm^3, with a Dmax of 25.15 Gy and a Dmin of 13.14 Gy. The Dmax on the left anterior descending (LAD) and on the circumflex arteries was 12.25 Gy. Tolerance doses for the remaining OARs were respected. Although VT burden decreased by 60 %, shocks were still delivered by the ICD, leading to a new CA 15 months after STAR, where a new VT morphology (VT-C) was induced (Fig. 1B), marginally different from VT-A. VT-C exited slightly more lateral compared to VT-A (towards segment 6) at the border of the previously irradiated zone, in an area poorly covered during the 1st STAR to respect the 12 Gy tolerance limit for the coronary arteries. Notably, 15 months after STAR a progression of his previously stable aortic stenosis was documented, possibly related to the first irradiation (Dmax 22.31 Gy and Dmean 8.22 Gy at this level).

The patient underwent a transcatheter aortic valve replacement and a redo STAR procedure targeting VT-C exit on May 5, 2020. A dose of 20 Gy at 82 % isodose was prescribed on this new volume of 3.7 cm^3. The dose delivered during the 1st STAR was also completed with a 15 Gy prescription over the initially irradiated volume. The cumulated Dmax on these two volumes were 31.01 and 32.63 Gy respectively, 16.79 Gy on the LAD and 19.39 Gy on the circumflex arteries. Over the 6 months after the 2nd STAR, VT burden dropped again, but some isolated VT episodes still persisted. Finally, 20 months after the second STAR, a slow VT was documented very similar to post-MI VT-B (Fig. 1C), hence away from both irradiated zones.

Case 2

A 61-year-old woman developed an electrical storm (ES) 6 years after an inferior MI (2013), that precipitated a cardiogenic shock successfully controlled with amiodarone. A double chamber ICD was implanted. Shortly thereafter she was admitted twice because of recurrent ES. The morphology of the clinical VT (VT-A) during CA suggested an exit at the infero-basal IVS (Fig. 2A), corresponding to a fibrotic infiltration (blue arrows) different from the infero-lateral MI scar seen on the MRI (yellow arrow). VT-A morphology could not be perfectly reproduced from the left or right IVS, nor from the coronary sinus, suggesting an intra-myocardial origin. A STAR was scheduled targeting the inferior third of the basal IVS (segments 2, 3 and 9) in order to encompass the exit site and part of the AS (Fig. 2A). On May 9, 2019 a dose of 20 Gy prescribed at 85 % isodose was delivered with a PTV of 25.54 cm^3, with a Dmax of 23.26 Gy and a Dmin of 19.37 Gy. The only OAR that received relevant doses was the stomach, with a Dmax of 12.59 Gy. Clinical follow-up showed a VT burden decrease of 95 % over the 1st 6 months and no ES recurrence. However, VTs recurred 6 months later and a 2nd CA was scheduled. The inducible VT (VT-B) was different from VT-A, with an exit at the infero-lateral MI region that was successfully ablated (segments 5 and 6) (Fig. 2B). The patient remained free from VT for 16 months until she was admitted for a new ES. Surprisingly, the ECG of this VT was comparable to VT-A. The EAM revealed an exit zone at the basal mid IVS (segments 2 and 3, Fig. 2C). Ablation from both side of the IVS (40 W, half-saline irrigation) failed to terminate VT-A due to its intra-myocardial location. Based on the fibrotic infiltration observed on the MRI, a 2nd STAR was performed on June 15, 2021 on a new PTV of 9.69 cm^3 targeting now the whole AS involved in VT-A (segments 2, 3, 8 and 9, Fig. 2C), upon which a dose of 22.5 Gy at 86 % isodose was prescribed. The dose delivered to the 1st PTV was completed with an additional 10 Gy (PTV of 30.71 cm^3) through a bias plan. Importantly, a transition volume localized between the other two received a dose of 15 Gy (PTV of 4.78 cm^3). The cumulated doses after these two treatments were Dmax 35.07 Gy and Dmean 32.97 Gy over the PTV; the LAD, the circumflex artery and the stomach cumulated Dmax values of 2.12, 5.17 and 21.72 Gy respectively. The patient remained free of VT for the next 6 months. No side effect related to re-irradiation was observed.

Discussion

VT are complex arrhythmias that can involve distinct substrates. Our patients had a history of MI, but also VT emerging from other LV segments related to non-ischemic myocardial scarring. Most importantly, these AS are often intramural such as within the IVS and/or at the basal anterior LV, and difficult to target with CA [8]. Hence, STAR appears as a valuable tool to treat such hidden AS.

Many aspects should be weighted in the analysis of these recurrences. Compared to other groups [4,9] our treatment volumes appear small. This might be related to the use of a Cyberknife, requiring less margins to adjust between GTV and PTV, as cardiac movements are tracked during the treatment. Additionally, our group aims to target only the clinical arrhythmias and not the whole arrhythmogenic substrate to limit toxicity, as exemplified by very low PTV values. As VT recurred at the border zone of previously irradiated regions as well as on previously known but non-irradiated AS, the question arises whether the first target volume should have covered all potentially AS to prevent late recurrences. Also, the transfer of information between the EAM and the radiation treatment planning software is indeed an important critical step and an unsolved issue [10]. Finally, the most appropriate radiation dose required to suppress VTs also remains unknown to date. At the time of the 1st STAR in our 2 patients only the clinical data from the group from St Louis had been published [1]. Our decision to administrate 20 Gy was based on the preclinical data, where a wide range of doses had been tried, from 5 to 160 Gy. More than a decade ago, overexpression of cardiomyocytes CX43 induced by STAR was reported to improve myocardial conduction and to decrease spatial heterogeneity of repolarization, rendering mice refractory to ventricular arrhythmias using heavy ion radiation with 5–15 Gy [11]. On the other hand, preliminary animal studies reported the occurrence of persistent conduction block and fibrosis with radiation doses >30 Gy [12,13], a value above the 20–25 Gy used in clinical practice [1,5,14]. It is therefore unlikely that the clinical benefit of STAR is only due to fibrosis of the VT substrate. These findings were confirmed by a recent study showing electrical conduction reprogramming involving Na$^+$ channel and CX43 overexpression as a possible antiarrhythmic mechanism before radiation-induced fibrosis occurs [15]. Herein, the administered 20 Gy might have been insufficient. However, both cases did not recur within the PTV. Our decision to re-treat the first PTV aimed at homogenizing the scar as animal studies showed more complete fibrosis with 35 Gy.

In summary, our 1st experience with redo STAR appears positive. However, data on early and late toxicities are still limited [16] and redo treatment should be reserved for highly selected patients.

Conclusion

These two cases show the feasibility of re-irradiation for uncontrollable VTs. No radiation toxicity was observed after the 2nd STAR with a follow-up of 19 and 6 months respectively. However, caution is advised as data on early and late toxicities remain scarce.

Informed consent statement

The two patients gave their written consent for publication of these cases.

Declaration of Competing Interest

The authors declare that they have no known competing financial interests or personal relationships that could have appeared to influence the work reported in this paper.

References

[1] Cuculich PS, Schill MR, Kashani R, Mutic S, Lang A, Cooper D, et al. Noninvasive cardiac radiation for ablation of ventricular tachycardia. N Engl J Med 2017;377 (24):2325–36.

[2] Neuwirth R, Cvek J, Knybel L, Jiravsky O, Molenda L, Kodaj M, et al. Stereotactic radiosurgery for ablation of ventricular tachycardia. Europace 2019;21:1088–95.

[3] Lloyd MS, Wight J, Schneider F, Hoskins M, Attia T, Escott C, et al. Clinical experience of stereotactic body radiation for refractory ventricular tachycardia in advanced heart failure patients. Heart Rhythm 2020;17(3):415–22.

[4] Gianni C, Rivera D, Burkhardt JD, Pollard B, Gardner E, Maguire P, et al. Stereotactic arrhythmia radioablation for refractory scar-related ventricular tachycardia. Heart Rhythm 2020;17(8):1241–8.

[5] Jumeau R, Ozsahin M, Schwitter J, Vallet V, Duclos F, Zeverino M, et al. Rescue procedure for an electrical storm using robotic non-invasive cardiac radio-ablation. Radiother Oncol 2018;128(2):189–91.

[6] Chin R, Hayase J, Hu P, Cao M, Deng J, Ajijola O, et al. Non-invasive stereotactic body radiation therapy for refractory ventricular arrhythmias: an institutional experience. J Interv Card Electrophysiol 2021;61(3):535–43.

[7] Benedict SH, Yenice KM, Followill D, Galvin JM, Hinson W, Kavanagh B, et al. Stereotactic body radiation therapy: the report of AAPM Task Group 101. Med Phys 2010;37(8):4078–101.

[8] Haqqani HM, Tschabrunn CM, Tzou WS, Dixit S, Cooper JM, Riley MP, et al. Isolated septal substrate for ventricular tachycardia in nonischemic dilated cardiomyopathy: incidence, characterization, and implications. Heart Rhythm 2011;8(8):1169–76.

[9] Knutson NC, Samson PP, Hugo GD, Goddu SM, Reynoso FJ, Kavanaugh JA, et al. Radiation therapy workflow and dosimetric analysis from a phase 1/2 trial of noninvasive cardiac radioablation for ventricular tachycardia. Int J Radiat Oncol Biol Phys 2019;104(5):1114–23.

[10] Boda-Heggemann J, Blanck O, Mehrhof F, Ernst F, Buergy D, Fleckenstein J, et al. Interdisciplinary clinical target volume generation for cardiac radioablation: multicenter benchmarking for the RAdiosurgery for VENtricular TAchycardia (RAVENTA) Trial. Int J Radiat Oncol Biol Phys 2021;110(3):745–56.

[11] Amino M, Yoshioka K, Tanabe T, Tanaka E, Mori H, Furusawa Y, et al. Heavy ion radiation up-regulates Cx43 and ameliorates arrhythmogenic substrates in hearts after myocardial infarction. Cardiovasc Res 2006;72:412–21.

[12] Blanck O, Bode F, Gebhard M, Hunold P, Brandt S, Bruder R, et al. Dose-escalation study for cardiac radiosurgery in a porcine model. Int J Radiat Oncol Biol Phys 2014;89(3):590–8.

[13] Zei PC, Wong D, Gardner E, Fogarty T, Maguire P. Safety and efficacy of stereotactic radioablation targeting pulmonary vein tissues in an experimental model. Heart Rhythm 2018;15(9):1420–7.

[14] Jumeau R, Vincenti MG, Pruvot E, Schwitter J, Vallet V, Zeverino M, et al. Curative management of a cardiac metastasis from lung cancer revealed by an electrical storm. Clin Transl Radiat Oncol 2020;21:62–5.

[15] Zhang DM, Navara R, Yin T, Szymanski J, Goldsztejn U, Kenkel C, et al. Cardiac radiotherapy induces electrical conduction reprogramming in the absence of transmural fibrosis. Nat Commun 2021;12:5558.

[16] Robinson CG, Samson P, Moore KMS, Hugo GD, Knutson N, Mutic S, et al. Longer term results from a phase I/II study of EP-guided noninvasive cardiac radioablation for treatment of ventricular tachycardia (ENCORE-VT). Internat J Radiat Oncol Biol Phys 2019;105(3):682.